Neutron scattering study of freezing in $Rb_{1-x}(ND_4)_xD_2PO_4$

H. Grimm,* K. Parlinski,† and W. Schweika
Kernforschungsanlage Jülich, Postfach 1913, D-5170 Jülich, West Germany

E. Courtens
IBM Zürich Research Laboratory, CH-8803 Rüschlikon, Switzerland

H. Arend
Eidgenössische Technische Hochschule Zürich—Hönggerberg, CH-8903 Zürich, Switzerland
(Received 23 July 1985; revised manuscript received 4 October 1985)

Crystals of the type $Rb_{1-x}(NH_4)_xH_2PO_4$ are frustrated due to the competing interactions of rubidium and ammonium which favor the ferroelectric and antiferroelectric configurations, respectively, within the hydrogen-bond system. The temperature, wave-vector, and frequency dependences of diffuse scattering are reported for a fully deuterated crystal of this type with an ammonium concentration of 62 mol%. Diffuse scattering streaks are observed along the ⟨100⟩ directions of the tetragonal crystal which peak at a wave vector that corresponds neither to the ferroelectric nor the antiferroelectric ordering of the pure crystals. Their intensity pattern in reciprocal space displays systematic extinction according to the odd representation of the group of this wave vector. The energy-resolved diffuse scattering has been analyzed as a superposition of an elastic, a quasielastic, and a very broad inelastic contribution. The quasielastic width decreases rapidly on cooling and cannot be resolved below 110 K.

INTRODUCTION

The freezing of randomly frustrated systems remains a subject of active debate. By far the broadest family under current study are spin-glasses, characterized by competing magnetic interactions.[1] There are, however, a number of advantages in investigating structurally frustrated systems. One of the advantages is that some measurements are possible in structural systems which are impossible or extremely difficult in the magnetic case, e.g., light scattering and x-ray diffuse scattering. Another reason to investigate structural glasses is of course that these model systems are a step closer to real topological glasses.

One excellent example of competing structural ordering are solid solutions of rubidium dihydrogen phosphate (RbH_2PO_4, or RDP) and ammonium dihydrogen phosphate ($NH_4H_2PO_4$, or ADP).[2] Those paraelectric crystals are isostructural at ambient temperature, with lattice constants that closely match, so that mixed crystals of $Rb_{1-x}(NH_4)_xH_2PO_4$ (or RADP) can be grown over the entire concentration range. Upon lowering the temperature, RDP becomes ferroelectric while ADP becomes antiferroelectric, related to different orderings of the acid-hydrogen bonds.[3] The ADP ordering is forced by the specific bonding of the ammonium protons which compete with the acid-proton bonding. Due to that competition, RADP maintains the overall paraelectric tetragonal structure, down to the lowest temperatures investigated, for $0.22 \lesssim x \lesssim 0.75$, but manifestations of freezing into glass are evident as high as 110 K.[2,4–12] Diffuse x-ray scattering results have already been obtained on concentrations near the ferroelectric (FE) side,[5] near the antiferroelectric (AFE) side,[6–9] and in the middle range of glass compositions.[6] They revealed a tendency to form superstructures of very-short-range order at intermediate concentrations, and diffuse scattering centered at the AFE Bragg peaks appeared close to the AFE phase boundary.

In summary, there seem to be aspects of the frustration both in time and space. On the one hand, methods which are insensitive to spatial correlations (e.g., dielectric response) show a dramatic increase of relaxation times on cooling. On the other hand, methods which are insensitive to time correlations (e.g., x rays) show the development of short-range order at wave vectors which correspond neither to the FE nor the AFE order parameter. Therefore, a simultaneous observation of the space *and* time dependence of the density-density correlations by thermal neutron scattering may provide additional insight into the dynamical origin of the freezing. Another motivation for this method is its sensitivity to the atoms whose correlations are expected to play a major role in this process, i.e., hydrogen or deuterium. In order to determine the distinct correlation function (correlation between different atoms) one has to use the deuterated salt because otherwise the self-correlation of hydrogen would dominate the scattering by its huge incoherent cross section.

The present paper reports the first coherent neutron-scattering results obtained on a crystal of the RADP family, namely $Rb_{0.38}(ND_4)_{0.62}D_2PO_4$. It should be noted that deuterated RDP can grow both in a tetragonal and in a monoclinic structure[13] and that the latter seems to be the stabler one. The experience gathered on the growth of deuterated RADP indicates that a small admixture of ammonium is sufficient to fully stabilize the tetragonal structure, isomorphic to that of protonated RDP and ADP.

As in all crystals of the KH_2PO_4 type, deuteration has a major effect on the characteristic ordering temperatures and on the dynamics. The Curie temperatures of tetragonal deuterated RDP and ADP are 218 K and 237 K, respectively,[14] while the corresponding values are 146 K and 148 K in the protonated salts. Independent dielectric constant measurements performed on a deuterated crystal of the composition used presently,[15] revealed that the frequency-dependent freezing temperature is close to 100 K at 10 MHz, and to 60 K at 1 KHz, while the Vogel-Fulcher freezing temperature is of the order of 26 K as opposed to 9 K for protonated crystals.[16] Finally, for undeuterated RADP the onset of freezing phenomena marked by the departure of a number of quantities from their usual lattice anharmonic behavior,[17] occurs near 110 K. For the deuterated salt, the corresponding temperature is not known but it is expected to be of the order of 200 K, which agrees with the onset of diffuse quasielastic intensity observed on cooling in the present experiment.

EXPERIMENTAL

RADP crystals, and their deuterated analogues, were prepared by means of a temperature-difference crystal-growth procedure working automatically at constant supersaturation. Equilibrated feed material is transported by thermal convection to a seed crystal grown previously by spontaneous nucleation from the same feed material and the corresponding solution. Details of the growth procedure will be published separately in connection with work covering crystal growth of solid-solution crystals exhibiting incommensurate phases.[18] The ammonium concentration was checked by x-ray diffraction determination of the a and c lattice parameter at ambient temperature. One finds $a=7.560$ and $c=7.440$ Å which, extrapolating the values of deuterated RDP and ADP and using the extensive knowledge accumulated on protonated RADP (Ref. 19) corresponds to $x=0.62\pm0.015$. The relative proton content was determined by NMR proton resonance on a large crystal, using a small undeuterated sample as reference. Taking account of the different relaxation times in both samples it was established that the deuteration in this crystal is superior to 99%.[20] The crystal (1.8 g/0.8 cm^3) had well-developed growth faces and was fully transparent with no indication of twinning. No broadening of the rocking curves could be detected. It was wrapped into aluminum foil, mounted into a He-filled sample cell with the c-axis vertical allowing thus for scanning the $(hk0)$ plane. In a second short run the a-axis was oriented vertically in order to complete the information about the intensity variation of the periodic diffuse scattering in the $(h0l)$ Brillouin zones. The sample cell was cooled by a closed cycle refrigerator.

The measurements were performed with a three-axis spectrometer. Pyrolitic graphite (002) reflections were used for the double monochromator and the analyzer together with a graphite filter placed in the incident beam which suppressed the higher-order contributions. Since the freezing affects drastically the widths of the scattering both in momentum and energy directions, and precise knowledge of the resolution was necessary for the data reduction. This was achieved within an average error limit of 2% by calibrating the resolution with standard scatterers (vanadium and Al_2O_3). The width of the vanadium scan was 0.249 ± 0.002 THz. It should be noted, however, that the resolution is a four-dimensional function in $(\mathbf{Q},\omega)$ space,[21] which cannot be presented by just one figure [$(\mathbf{Q},\omega)$ are defined by $\mathbf{Q}=\mathbf{K}_i-\mathbf{K}_f$ and $\omega=\frac{1}{2}(K_i^2-K_f^2)$, where $\mathbf{K}_i,\mathbf{K}_f$ denote the incident and final wave vector of the neutron)]. The effect of the resolution broadening depends therefore on the type of the scattering function and on the direction of the scan in $(\mathbf{Q},\omega)$ space. Whenever necessary, this effect is indicated below for specific scans and specific assumptions about the scattering function.

DIFFUSE SCATTERING AT LOW TEMPERATURES

A preliminary survey with a diffuse scattering spectrometer has revealed diffuse peaks within the (110) Brillouin zone at low temperatures which were not visible in the map taken at room temperature. The aim of the triple axis measurements was to study these peaks in more detail and to resolve eventually their quasielastic broadening.

Figures 1(a) and 1(b) display the shape of these diffuse peaks in the (303) and (240) zone, respectively. They peak at about $0.35a^*$ ($a^*=2\pi/a$) and are "cigar shaped" with the long axis in the (100) direction. They are asymmetric in this direction, showing a smoother decay versus the Z points ($h+k=$odd, $l=$even and vice versa). For our concentration of $x=0.62$, no antiferroelectric short-range-order peaks are recognizable at these points, in agreement with the independent results of Cowley *et al.*[6] obtained from the nondeuterated analogue. The widths perpendicular to the long axis are similar, the width along the c axis being about 20% broader (without resolution correction). Scanning the energy direction at the peak position did not show any inelasticity at these temperatures (i.e., 14 and 39 K) within our resolution. Actually the width of such a scan is somewhat smaller compared to the calibration scan from vanadium since the "dimensionality" of the scattering function in momentum space is lower than three due to the cigar shape. The intensity shows a remarkable variation changing from $\mathbf{q}$ to $-\mathbf{q}$ especially along the $\mathbf{k}$ direction in the Brillouin zone (240) displayed in Fig. 1(b).

In order to look for any systematic variation in the intensity of these peaks we mapped out a quarter of the accessible circle $h^2+k^2\lesssim5.2$, $l=0$ in steps of $a^*/3$. This map shows (i) that the asymmetry with respect to $\mathbf{q}$ is observable in many Brillouin zones, (ii) that the stronger peak has not systematically a larger distance from the origin, (iii) that there are no peaks for h or k equal to zero, and (iv) that the peak pattern has mirror symmetry with respect to the (110) axis. Figure 2 displays this intensity information qualitatively. Because of the mirror symmetry only two "satellites" are shown per Brillouin zone. This map provided the "background" variation as well, which smoothly decreases with increasing momentum Q. The decay gives some idea about the average dislocation in this system and would result in $u^2\simeq0.03$ Å^2 if

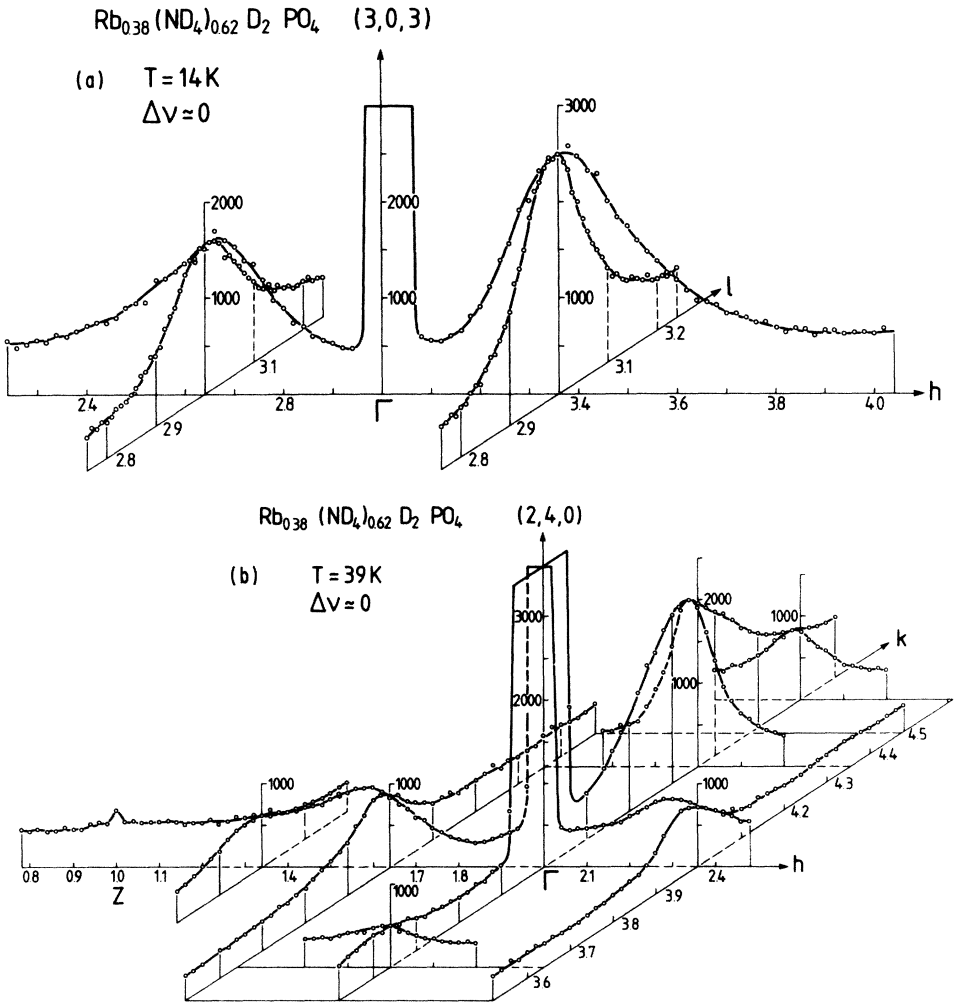

FIG. 1. (a) Intensity of the diffuse scattering close to the reciprocal-lattice vector (303) at 14 K. The abscissae h,k,l refer to the tetragonal unit cell. (b) Same as (a) close to (240) at 39 K.

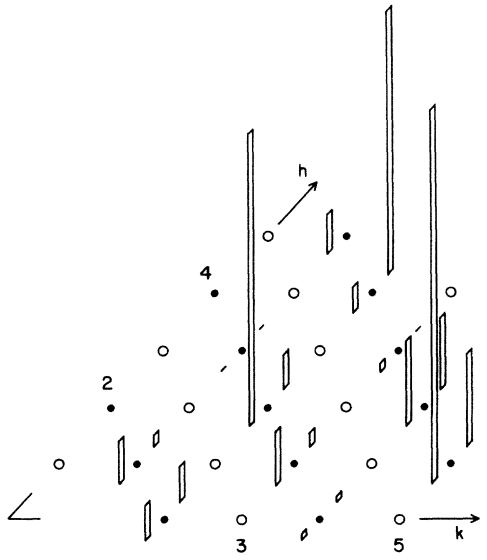

FIG. 2. Map of the peak intensities of the periodic diffuse pattern in the $(hk0)$ plane at 14 K. Only two values are shown per reciprocal-lattice vector. The second pair is related by mirror symmetry around the twofold (110) axis.

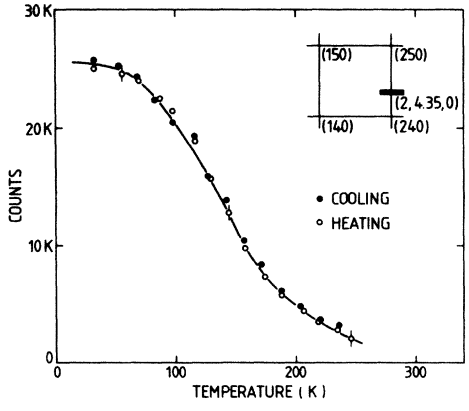

FIG. 3. Integrated elastic (spectrometer set to $\omega=0$) intensity of the scan $(1.7<\xi<2.3, 4.35, 0)$ across the diffuse streak obtained with a constant cooling (●) and heating (○) rate of 10 K/h. The background is subtracted by extrapolation and amounts to about 20% of the peak intensity at 32 K. The inset indicates the scan path.

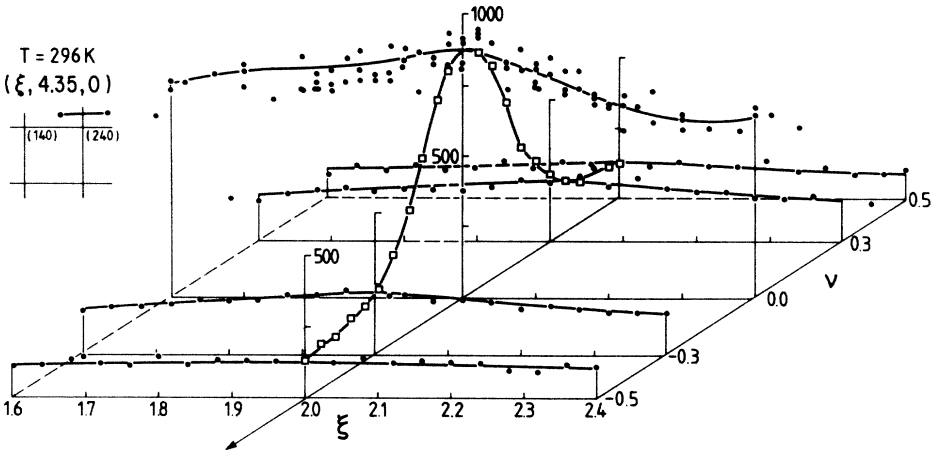

FIG. 4. Onset of the localized diffuse scattering at $Q=(2,4.35,0)$ at 296 K together with its energy variation (ν in units of THz). The inset indicates the scan path in Q space.

described in the manner of a Debye-Waller factor. This value is compatible with that of locked-in acid protons in pure potassium dihydrogen phosphate in the ferroelectric phase.[22] It seems that the diffuse scattering can be divided into one part which reflects the average symmetry of the crystal (cigar-shaped scattering in q space) and a smoothly varying background in Q space ($\mathbf{Q}=\mathbf{G}+\mathbf{q}$, where G is a reciprocal-lattice vector). Whatever "eigenvector" is chosen in order to describe the pattern of Fig. 2, it must also involve displacements along the fourfold axis since drastic intensity variations along l were observed in the $(h0l)$ plane too. Intense satellites were observed, e.g., in the (004) Brillouin zone as well.

TEMPERATURE VARIATION OF THE DIFFUSE SCATTERING

On heating and cooling at a rate of 10 K/h a series of scans were made at $\mathbf{Q}=(2,4.35,0)$ along the h direction with the energy transfer ω being set to zero. The area of this section through the diffuse peak is displayed in Fig. 3 after subtracting the background. The background increases by about a factor of 2 on going from 32 to 250 K. No hysteresis is observed. The temperature range within which the integrated intensity changes is very broad, i.e., from about 40 to 250 K. The peak is still recognizable at room temperature as can be seen from Fig. 4 which displays in addition the energy variation. The observed energy width of 0.29 THz at this temperature is clearly larger than the width of 0.25 THz which was observed for the Q-independent elastic scatter (vanadium), thus proving that there develops a quasielastic component at high temperatures. Another cause affecting this integrated intensity seems to be a slight shift towards the Z point at higher temperatures as demonstrated in Fig. 5. This figure corresponds to Fig. 1(b) changing the temperature from 39 to 155 K. The strongest satellite at (2,4.35,0) has become very flat for $4.25<k<4.5$. A similar behavior was observed by Cowley *et al.*[6] with x rays for the nondeuterated compound. A fourth "leakage" of the peak intensity on heating is the broadening of the width perpendicular to the "cigar" which is observable in the raw data above say 110 K.

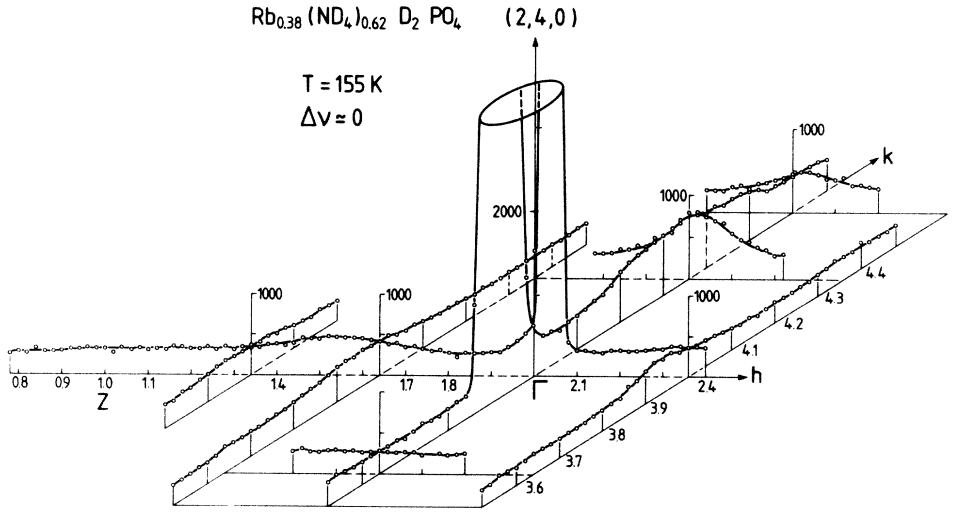

FIG. 5. Same as Fig. 1(b) at a temperature of 155 K.

In order to disentangle all these variations we analyzed three types of scans *simultaneously* as a function of temperature with the resolution which was independently fitted to the Al_2O_3 and Va data. The three types of scans were $(2\pm x, 4.35, 0, 0)$, $(2,4.35,0,x)$, and $(2.6,3.65,0,x)$ in (h,k,l,ω) space, where x denotes the scan variable, (h,k,l) are Miller indices, and ω represents the energy transfer. The third scan represents an arbitrary point in the Brillouin zone with a momentum Q similar to the point of interest which is free from Debye-Scherrer line contributions and thus informed about the background-variation.

Analysis of this latter variation resulted in no detectable quasielastic component within our resolution. Consequently, the scattering function was represented by

$$S(\mathbf{Q},\omega)\sim I_1\delta(\omega)+I_2 ,$$

folded with the resolution at each point of the scan $(2.6, 3.65, 0, |x| \leq 0.4$ THz) and fitted to the experimental data. The resulting temperature dependences of I_1 and I_2 are shown in Fig. 6. The increase (decrease) of the inelastic (elastic) scattering becomes noticable between 40 and 60 K.

The additional cigar-shaped diffuse peak at (2,4.35,0,0) was modeled by a normalized, orthogonal, four-dimensional Gaussian with the prefactor I_3 centered at this location. Cylindrical symmetry was assumed around the long axis and the full width at half maximum (FWHM) along k was set to 0.2 Å^{-1}. These two assumptions do not affect the analysis in an essential way because of the relaxed vertical resolution and the cigar being much longer than the resolution ellipsoid. The parameters fitted to the series $(2\pm x, 4.35, 0, 0)$ and $(2,4.35,0,x)$ were the intensity I_3 of the Gaussian, the momentum width perpendicular to the long axis and the energy width. The $(2\pm x, 4.35, 0, 0)$ scans demanded a Lorentzian decay in this direction which was to sufficient accuracy approximated by splitting the Gaussian into two Gaussians with no additional parameter. Actually the $(2\pm x, 4.35, 0,)$ scans seemed to decay somewhat slower than Lorentzian at low temperatures and the $(2,4.35,0,x)$ scans somewhat steeper than Gaussian at high temperatures. The Gaussian representation was maintained in view of the convenient folding with the resolution and the statistical errors.

Figures 7(a) and 7(b) show the result of this simultaneous fit for the momentum and energy widths. Below about 110 K the FWHM in q is stable at 0.086 Å^{-1},

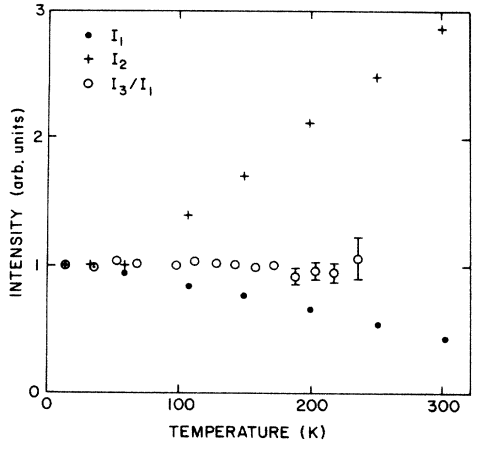

FIG. 6. Temperature variation of intensities as obtained from the resolutions analysis. I_1 (●) represents the elastic intensity at arbitrary point (2.6,3.65,0). $(+)=I_2$ represents the inelastic, frequency independent (≤ 0.5 THz) intensity at the same point including the instrumental background. Its upper estimate of two counts per minute would account for 50% of I_2 at 0 K. I_3/I_1 (○) represents the ratio of diffuse peak intensity, integrated over q and ω, to elastic intensity at arbitrary point with similar Q. All three intensities are normalized to unity at 0 K.

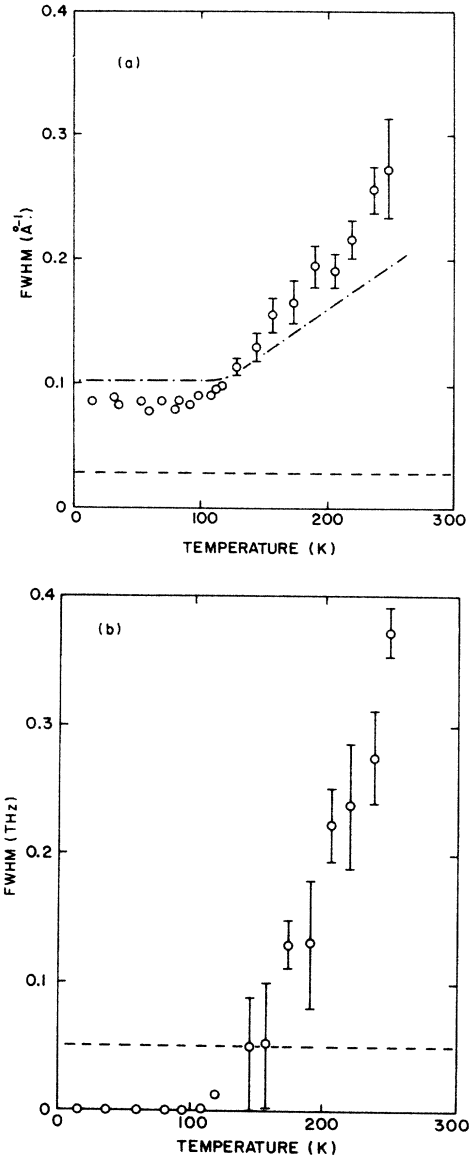

FIG. 7. (a) Temperature variation of the correlation length (2/FWHM) perpendicular to the diffuse cigar at (2,4.35,0) as obtained from the resolution analysis. The dot-dashed line indicates the results from the raw data. The dashed line corresponds to the experimental width of an infinitely thin cigar. (b) Energy width of the quasielastic scattering at (2,4.35,0) as obtained from the resolution analysis. The dashed line indicates the limit at which the fit recognizes a genuine energy width.

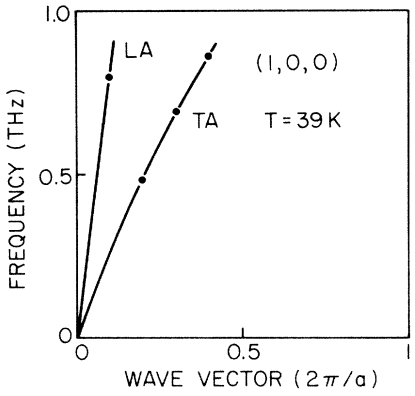

FIG. 8. Acoustic phonon branches with polarization vectors within the $(h,k,0)$ plane at 39 K.

which corresponds to a correlation length at 23 Å or three lattice constants or six hydrogen bonds. Above 110 K the width increases rapidly and around 250 K there remains merely a next-neighbor correlation in terms of acid protons. A similar behavior is observed in the energy width yet with the difference that the fit cannot "recognize" any width ≤ 0.05 THz [indicated by the dashed line in Fig. 7(b)]. Within this limitation the scattering is elastic below 110 K and broadens rapidly above. We checked whether the two acoustic branches, polarized within the scattering plane, are affected by this process and got a negative answer within our intensity and resolution limits. The results are displayed in Fig. 8. The branches soften by about 10% at room temperature but no anomaly at $0.35a^*$ is observed for the TA branch. The slopes are similar to KD_2PO_4.[23] The integrated [in $(\mathbf{q},\omega)$ space] intensity of the diffuse peak (I_3) is compared with the average elastic scattering (I_1) in Fig. 6. Within the accuracy of the fit the ratio I_3/I_1 is independent of temperature which means that the additional dislocation of atoms caused by heating the sample affects both types of scattering in the same way. No discontinuity is observed around 110 K or below.

DISCUSSION OF INTENSITY PATTERN

The observation of the diffuse scattering periodically peaked at the star of $\mathbf{q}\approx\mathbf{a}^*/3$ is reminiscent of the order parameter fluctuations of the ordinary phase transitions in the translationally invariant crystals. The limiting concentration $x=1$ shows cigar-shaped critical scattering elongated along the $\bar{4}$ axis and peaked at the Z point ($\mathbf{q}=\mathbf{a}^*$) characteristic for the antiferromagnetic correlations in the a-b plane.[24] This type of scattering has been observed also for $x=0.70$,[9] and Cowley *et al.*[6] showed that it gradually vanishes in the "glassy" phase on changing x from 0.78 to 0.68, whereas the scattering under discussion increases with a tendency to shift to smaller wave vectors. At the other extreme ($x=0$) one observes critical fluctuations around the Γ point ($\mathbf{q}=0$) characteristic for the uniaxial ferroelectric properties.[23,25] Their asymmetric appearance in the $(hk0)$ planes was successfully explained by their coupling to the acoustic modes.[26] For $x=0.35$ Courtens *et al.*[5] observed diffuse peaks at about $\mathbf{a}^*/4$.

The experimental evidence is therefore that the Σ line ($\mathbf{q}_\Sigma=2\mu\mathbf{a}^*$, $0<\mu<0.5$) offers wave vectors which are to a certain extent "preferred" by the low-frequency excitations of the mixed system. The symmetry and the systematic extinction of the peaks for $l=0$ and h or k equals zero suggests the examination of the constraints on eigenvectors along the Σ line in space group $I\bar{4}2d$.

This group-theoretical analysis refers, of course, to a fictitious translationally invariant crystal with interactions and scattering lengths averaged over the Rb and ND_4 distribution. Questions to this analysis are, whether these exists an irreducible representation which is compatible with both the FE- and the AFE-type ordering of the acid protons and, if so, whether it produces the observed extinction. Finally, the analysis might give some hint to the origin of the strong dependence of the intensity of the diffuse peaks on the sign of the wave vector $\mathbf{q}$. The following discussion is restricted to the displacements of the acid protons and only the intensities for $\mathbf{Q}=2\pi(h,k,0)$ are considered.

The primitive cell contains four such protons and one may select, e.g., those four hydrogen bonds attached to the PO_4 group centered at $(0,\frac{1}{2},\frac{1}{4})$ (components refer throughout to the tetragonal unit cell). Their average positions are

$$\mathbf{X}(1)=(u,\tfrac{1}{2}-\tfrac{1}{4},\tfrac{1}{8}),\quad \mathbf{X}(3)=(\tfrac{1}{4},\tfrac{1}{2}+u,\tfrac{3}{8}),$$

$$\mathbf{X}(2)=(-u,\tfrac{1}{2}+\tfrac{1}{4},\tfrac{1}{8}),\quad \mathbf{X}(4)=(-\tfrac{1}{4},\tfrac{1}{2}-u,\tfrac{3}{8}),$$

with $u\approx\frac{1}{7}$. The group of the wave vector $\mathbf{q}_\Sigma=4\pi\mu(1,0,0)$ has the twofold axis only besides the identity giving rise to an odd and an even representation. The corresponding (4×3)-component eigenvectors are[27]

$$\mathbf{E}_{\text{even}}=(\alpha_1,\underline{0},0\,|\,\alpha_1^*,\underline{0},0\,|\,\underline{a}_3\epsilon,ia_4\epsilon,a_5\epsilon\,|\,\underline{a}_3\epsilon^*,-ia_4\epsilon^*,-a_5\epsilon^*),$$

$$\mathbf{E}_{\text{odd}}=(0,\underline{\beta}_1,\beta_2\,|\,0,-\underline{\beta}_1^*,\beta_2^*\,|\,\underline{b}_5\underline{\epsilon},ib_6\epsilon,b_7\epsilon\,|\,-\underline{b}_5\underline{\epsilon}^*,ib_6\epsilon^*,b_7\epsilon^*),$$

where $\epsilon=\exp(i\pi\mu)$. The other quantities denote arbitrary functions of μ and Greek symbols are used if they are complex. The restriction to real functions for the hydrogen bonds parallel to $\mathbf{q}_\Sigma$ [i.e., $\mathbf{X}(3),\mathbf{X}(4)$] is a consequence of time invariance. The displacements along the hydrogen bonds are underlined. For $\beta_1=b_5=1$ at both the Γ and the Z point the eigenvector $\mathbf{E}_{\text{odd}}$ is indeed compatible with the ferroelectric and antiferroelectric proton arrangement.

The "visibility" of an eigenvector $\mathbf{E}=[\mathbf{e}(1)\,|\,\mathbf{e}(2)\,|\,\cdots]$ in $\mathbf{Q}$ space is governed by the dynamical structure factor

$$F^*(\mathbf{Q})\sim\sum_\kappa \mathbf{Q}\cdot\mathbf{e}(\kappa)\exp[-i\mathbf{Q}\cdot\mathbf{x}(\kappa)],$$

where scattering length and Debye-Waller factor have been omitted for simplicity. Restricting to the $(hk0)$ plane, one has

$$\mathbf{Q}=\mathbf{G}+\mathbf{q}_\Sigma=2\pi(H+2\mu, K, 0) ,$$

with the integers H, K, and $H+K$ being even. Including the motions along the hydrogen bonds only ($b_6=0$) one gets for the $\mathbf{E}_{\text{odd}}$ contribution

$$F_{\text{odd}}(\mathbf{Q})\sim Kr\sin[2\pi(\phi+Hu-K/4)] + (H+2\mu)\sin[2\pi(H/4+Ku)] ,$$

where β_1 and b_5 have been replaced by r and ϕ with

$$\beta_1/b_5=r\exp[i2\pi(\phi-2\mu u)] .$$

It is readily seen that F_{odd} vanishes for $K=0$ since then H has to be even (Fig. 2). This extinction is independent of the restriction $b_6=0$ and is not valid for F_{even}. Switching to the opposite arm of the star of $\mathbf{q}_\Sigma$ changes the sign of μ and ϕ. The sign of μ influences F_{odd} only weakly whereas the phase lag ϕ between the upper and lower hydrogen displacements offers the possibility of a large asymmetry with respect to the Γ point.

Considering the scarcity of the presently available data and the simplifications of the argument above, one cannot expect to extract quantitative informations from the observed intensities. On the one hand, the crystal is strongly bond disordered; on the other hand, one has to allow for the displacements of the other atoms, as well (e.g., distortion of the oxygen tetrahedron in the x,y plane, orientation and translation of the NH_4 groups).

SUMMARY AND DISCUSSION

Elastic and inelastic scattering of thermal neutrons by a mixed crystal of type $Rb_{1-x}(ND_4)_xD_2PO_4$ has been investigated for a concentration ($X=0.62$) which displays no long-range order transition nor short-range antiferroelectric correlations. The following results were obtained:

(1) Cigar-shaped peaks, arising from distinct correlations, elongated along the line joining the wave vectors of the ferroelectric and antiferroelectric order parameters and peaked at about $\mathbf{a}^*/3$ are observed.

(2) This scattering develops within our energy resolution a time persistent part which grows smoothly on cooling and saturates at about 30 K (Fig. 3). The inflection point for the raw data is at about 130 K.

(3) The resolution correction reveals that actually at about 110 K the energy width becomes indistinguishably small [Fig. 7(b)]. It suggests that any anomalous temperature dependence vanishes on integration of the diffuse peak over $\mathbf{q}$ and ω (Fig. 6). Thus the x-ray scattering "sees" an anomalous temperature dependence only via the change of correlation length in $\mathbf{q}$ space [Fig. 7(a)]. A similar effect on energy integration has been observed by Aeppli *et al.*[28] for amorphous MnSi.

(4) The self-correlation-type scattering observed at an arbitrary point of the Brillouin zone shows a broad (scan is -0.5 THz $<\omega/2\pi<0.5$ THz) inelastic and an elastic contribution. The temperature dependence of the elastic contribution is within error limits the same as that of the $(\mathbf{q},\omega)$-integrated diffuse peak (Fig. 6, I_1, I_3/I_1). A possible quasielastic scattering could not be identified due to resolution-intensity limitations.

(5) The intensity pattern of the diffuse peaks in $\mathbf{Q}$ space (Fig. 2) displays extinction characteristic of the odd representation of the Σ line. A possible reason for the sometimes large asymmetry with respect to the relevant Γ point is a phase lag or a distribution of phase lags between the upper and lower hydrogen bonds attached to a PO_4 group. The correlation length perpendicular to the Σ line saturates at about six hydrogen bonds below 110 K.

It is expected that the investigated system has some similarity with the soft spin version of the Edwards-Anderson model, whose relaxational dynamics have been discussed by Sompolinsky and Zippelius[29] in the mean-field limit. According to their analysis, the relaxation rate for the self-correlation of the spin fluctuations should display a critical slowing down for a finite temperature. No predictions are made for the distinct correlation function because of the restriction to a symmetric distribution of the random interaction.

We did not observe a quasielastic component for the background scan, which should contain the virtually $\mathbf{q}$-independent scattering due to the self-correlation. We rather observed a broad continuum of states (intensity I_2 in Fig. 6). On the other hand, we did observe a critical slowing down for the diffuse peaks, which correspond to distinct correlations because of their $\mathbf{q}$ dependence. Possible reasons for this difference are resolution limitations and/or the relative weakness of the self-correlation contribution. Note that this contribution is spread out over the whole Brillouin zone and superimposed on a large genuinely elastic contribution due to the disorder in the scattering lengths, introduced by the random distribution of Rb and ND_4.

The location of the diffuse peaks in $\mathbf{q}$ space is not understood. A hint is given by molecular dynamics calculations for a simplified RADP model.[30] Adjusting the interaction such that an AFE (a FE) transition takes place for the pure ND_4(Rb) salt, there arise diffuse peaks between the Γ and the Z point for intermediate concentrations, very similar to the experiment. They peak at the crossing of the lowest dispersion branches for the pure salts. These branches are of relaxational type and transform according to the odd representation of $\mathbf{q}_\Sigma$.

ACKNOWLEDGMENTS

Fruitful comments by T. Springer, S. Shapiro, and G. Aeppli are gratefully acknowledged. We thank R. A. Cowley for the information about the x-ray results prior to publication. We are also grateful for the effective technical assistance of K. Schönknecht. One of us (K.P.) would like to thank the staff of the Institut für Festkörperforschung, Kernforschungsanlage Jülich, and another of us (H.G.) thanks Brookhaven National Laboratory for their hospitality and assistance.

*Permanent address: Institute of Nuclear Physics, ulica Radzikowskiego 152, PL-31-342 Krakow, Poland.
†Present address: Physics Department, Brookhaven National Laboratory, Upton, NY 11973.

[1]For recent reviews, see e.g., K. H. Fischer, Phys. Status Solidi B **116**, 357 (1983).
[2]E. Courtens, J. Phys. (Paris) Lett. **43**, L199 (1982).
[3]J. C. Slater, J. Chem. Phys. **9**, 16 (1941).
[4]E. Courtens, Helv. Phys. Acta **56**, 705 (1983).
[5]E. Courtens, T. F. Rosenbaum, S. E. Nagler, and P. M. Horn, Phys. Rev. and P. M. Horn, Phys. Rev. B **29**, 515 (1984).
[6]R. A. Cowley, T. Ryan, and Eric Courtens, J. Phys. C **18**, 2793 (1985).
[7]S. Iida and H. Terauchi, J. Phys. Soc. Jpn. **52**, 4044 (1983).
[8]H. Terauchi, T. Futamura, Y. Nishita, and S. Iita, J. Phys. Soc. Jpn. **53**, 483 (1984).
[9]S. Hayase, T. Futamura, H. Sakashita, and H. Terauchi, J. Phys. Soc. Jpn. **54**, 812 (1985).
[10]J. Slak, R. Kind, R. Blinc, E. Courtens, and S. Zumer, Phys. Rev. B **30**, 85 (1984).
[11]E. Courtens, Phys. Rev. Lett. **52**, 69 (1984).
[12]E. Courtens and H. Vogt, J. Chim. Phys. **82**, 317 (1985).
[13]N. S. J. Kennedy and R. J. Nelmes, J. Phys. C **13**, 4841 (1980).
[14]See, e.g., *Ferroelectrics and Related Substances*, Vol. 16 of *Landolt-Börnstein*, edited by K.-H. Hellwege and A. M. Hellwege (Springer-Verlag, Berlin, 1982), pp. 83 and 88.
[15]E. Courtens (unpublished).
[16]E. Courtens and H. Vogt, Z. Phys. B. (to be published)
[17]E. Courtens, Proceedings of the NATO Advanced Study Institute on Scaling Phenomena in Disordered Systems, Geilo, 1985 (unpublished).
[18]H. Arend, H. Wüest, R. Perret, and P. Kerkoč, J. Cryst. Growth (to be published).
[19]E. Courtens, Jpn. J. Appl. Phys. (to be published).
[20]One of us (E.C.) express many thanks to Dr. Mali, University of Zurich, for performing this titration.
[21]M. J. Cooper and R. Nathans, Acta Crystallogr. **23**, 357 (1967).
[22]H. Grimm, H. Stiller, and Th. Plesser, Phys. Status Solidi **42**, 207 (1970).
[23]J. Skalyo, Jr., B. C. Frazer, and G. Shirane, Phys. Rev. B **1**, 278 (1970).
[24]H. Meister, J. Skalyo, Jr., B. C. Frazer, and G. Shirane, Phys. Rev. **184**, 550 (1969).
[25]W. J. L. Buyers, R. A. Cowley, G. L. Paul, and W. Cochran, *Neutron Inelastic Scattering* (IAEA, Vienna, 1968), Vol. I, p. 267.
[26]R. A. Cowley, Phys. Rev. Lett. **36**, 744 (1976).
[27]For the definition of the projection operator see, e.g., A. A. Maradudin and S. H. Vosko, Rev. Mod. Phys. **40**, 1 (1968).
[28]G. Aeppli, J. J. Hansen, G. Shirane, and Y. J. Uemura, Phys. Rev. Lett. **54**, 843 (1985).
[29]H. Sompolinsky and A. Zippelius, Phys. Rev. B **25**, 6860 (1982).
[30]K. Parlinski and H. Grimm (unpublished).